Tuning a Coiled-coil Hydrogel *via* Computational Design of Supramolecular Fiber Assembly

Dustin Britton[†], *Michael Meleties*[†], *Chengliang Liu*[†], *Sihan Jia*[†], *Farbod Mahmoudinobar*[†‖], *P. Douglas Renfrew*[‖], *Richard Bonneau*[‖,⊥,#], *and Jin Kim Montclare*[†,¶,∇,°*]

† Department of Chemical and Biomolecular Engineering, New York University Tandon School of Engineering, Brooklyn, New York, 11201, USA

‖. Center for Computational Biology, Flatiron Institute, Simons Foundation, New York, New York, 10010, USA

⊥. Center for Genomics and Systems Biology, New York University, New York, New York, 10003, USA

#. Courant Institute of Mathematical Sciences, Computer Science Department, New York University, New York, New York, 10009, USA

¶ Bernard and Irene Schwartz Center for Biomedical Imaging, Department of Radiology, New York University School of Medicine, New York, New York, 10016, USA

∇ Department of Chemistry, New York University, New York, New York, 10012, USA

° Department of Biomaterials, New York University College of Dentistry, New York, New York, 10010, USA

* Corresponding author

Email: montclare@nyu.edu

SUPPORTING INFORMATION

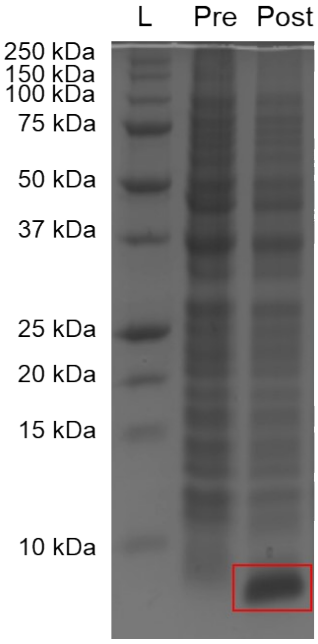

Figure S1. Q2 protein (6.48 kDa) after expression. L: Ladder, Pre : Pre induction with IPTG, Post: Post-induction with IPTG

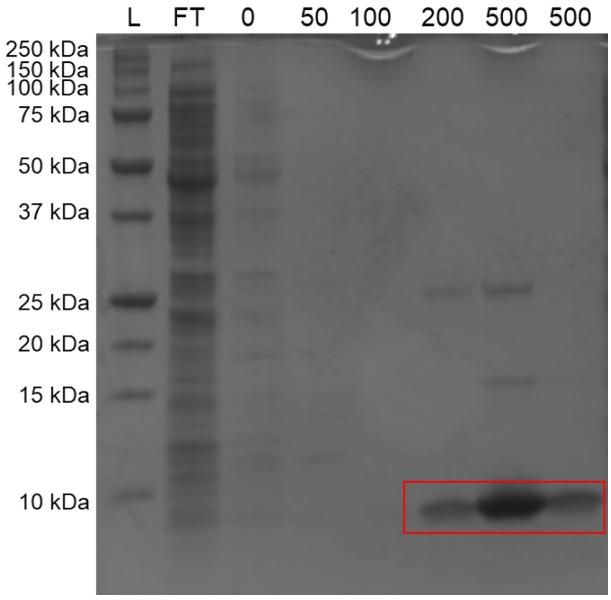

Figure S2. Q2 protein (6.48 kDa) after purification. L: Ladder, FT : Flow-through, following are increasing mM concentrations of imidazole

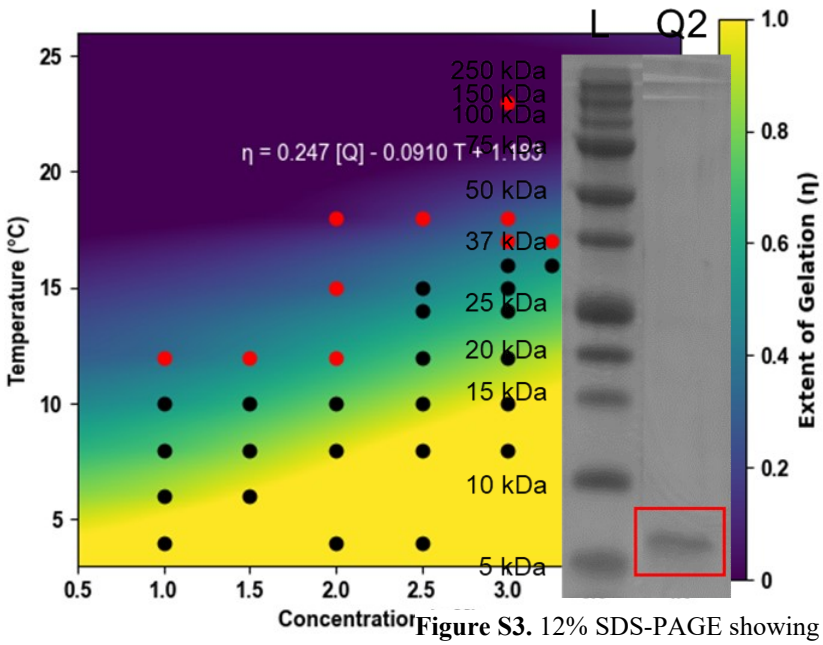

Figure S3. 12% SDS-PAGE showing > 99% purity of final Q2 protein (6.48 kDa) after dialysis and concentration to 2 mM. Lanes cropped and moved together without resizing. Original available upon request.

Figure S4. Extent of gel… r regression of a concentration-temperature… tube inversions showing gel behavior (bl… olution behavior (red dots) after two weeks … from Hill *et al*.[1]

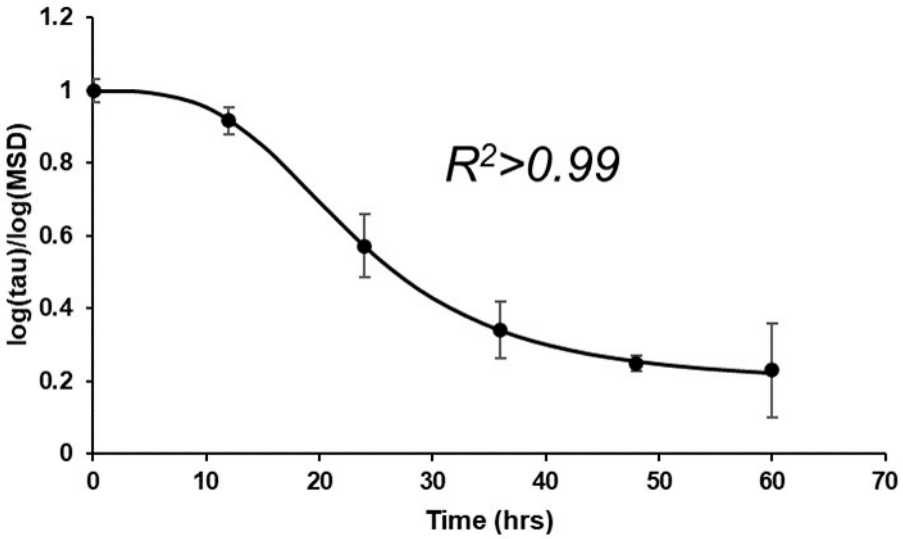

Figure S5. Sigmoidal fit solved in MATLAB. Data is represented as the average and standard deviation of three independent trials. Logarithmic plateaus at the start and end of the curve used to determine solution and gelation equilibration.

Figure S6 a. Log-log plot of MSD and lag time, τ, for independent trial (no. 2) of Q2 determined by MPT. **b**. Time-cure superposition of MSD vs τ. **c**. Logarithmic shift factors for the vertical (log(a) in blue) and horizontal (log(b) in red) directions used in the time cure superposition to the determine the t_{gel}. **d**. Log-log plot of the shift factors and their distance from the t_{gel}, determined by the ratio of the logarithmic slopes of the horizontal to vertical shift factor.

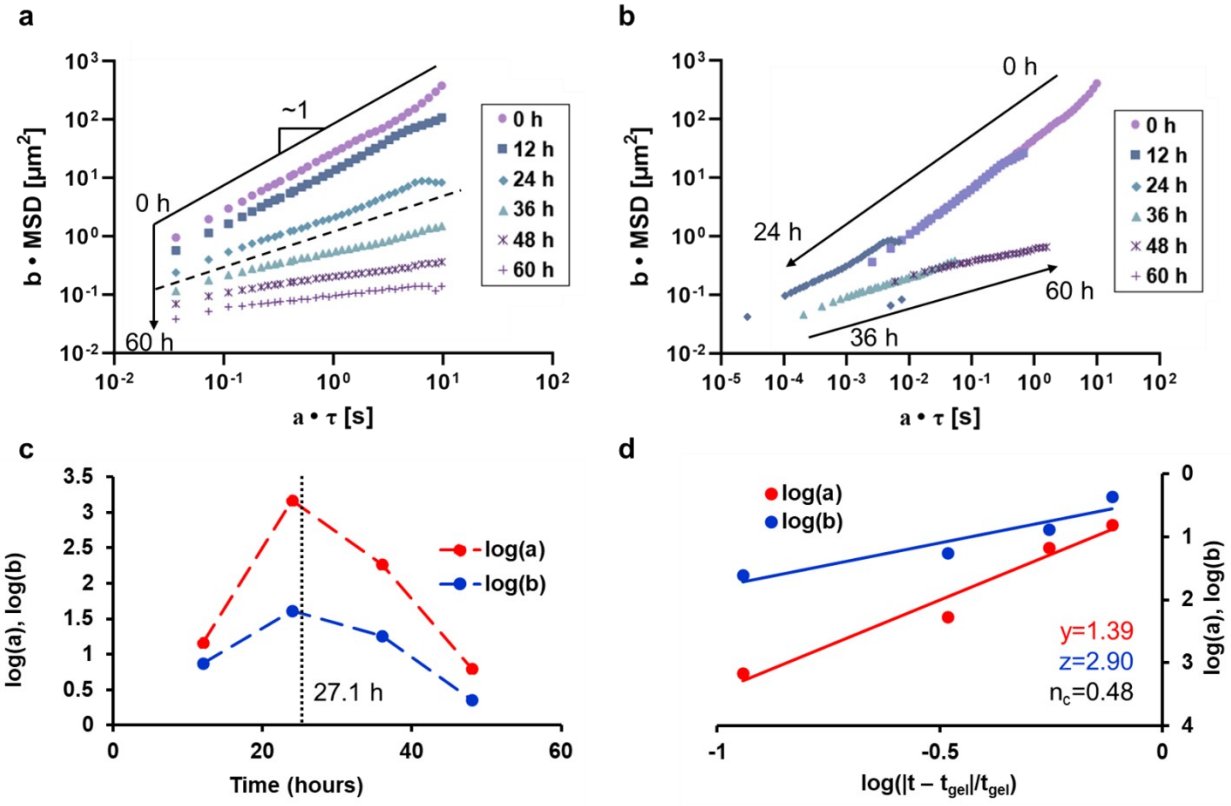

Figure S7 a. Log-log plot of MSD and lag time, τ, for independent trial (no. 2) of Q2 determined by MPT. **b**. Time-cure superposition of MSD vs τ. **c**. Logarithmic shift factors for the vertical (log(a) in blue) and horizontal (log(b) in red) directions used in the time cure superposition to the determine the t_{gel}. **d**. Log-log plot of the shift factors and their distance from the t_{gel}, determined by the ratio of the logarithmic slopes of the horizontal to vertical shift factor.

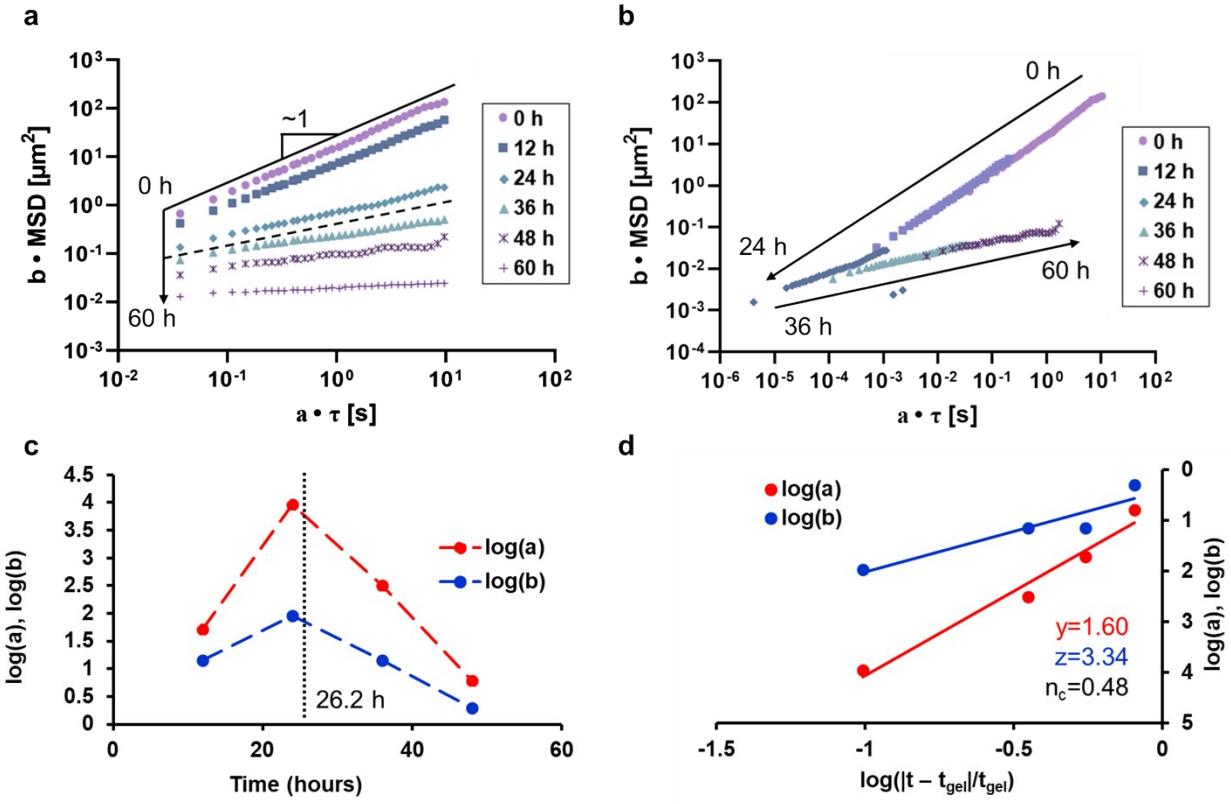

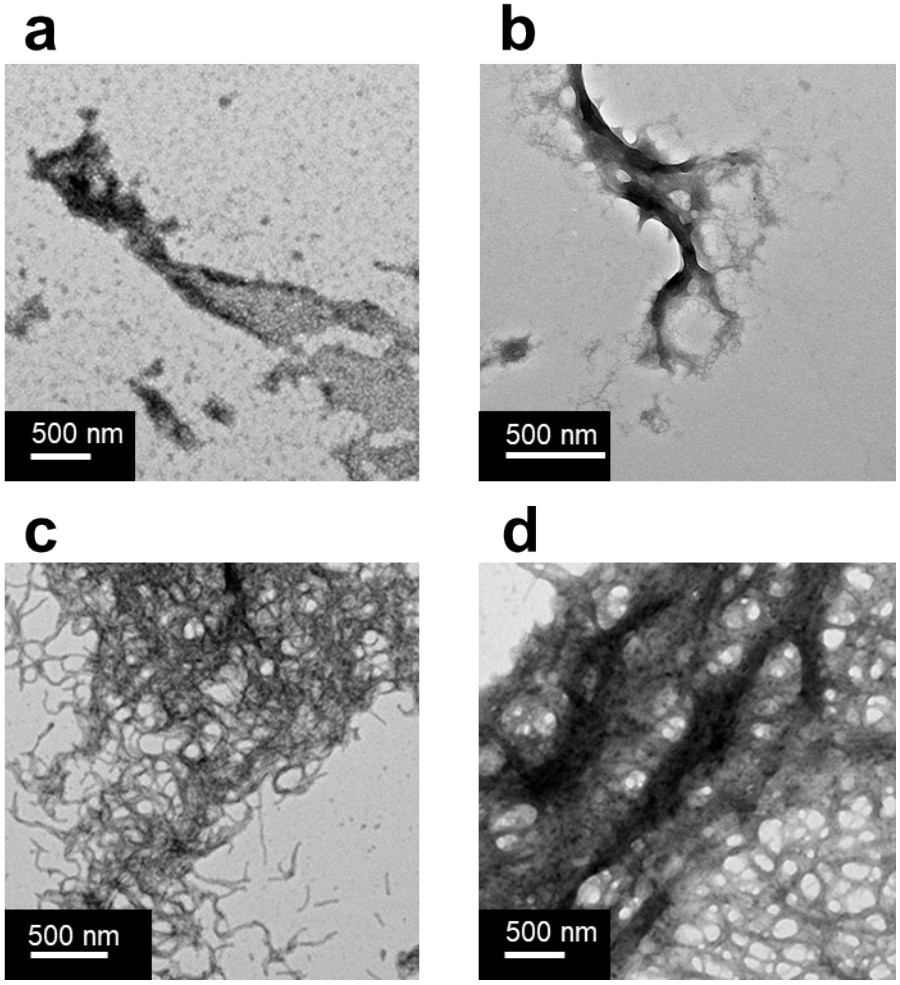

Figure S8 TEM images of Q at times **a.** 0 h, **b.** 24 h, **c.** 84 h, and **d.** 144 h.

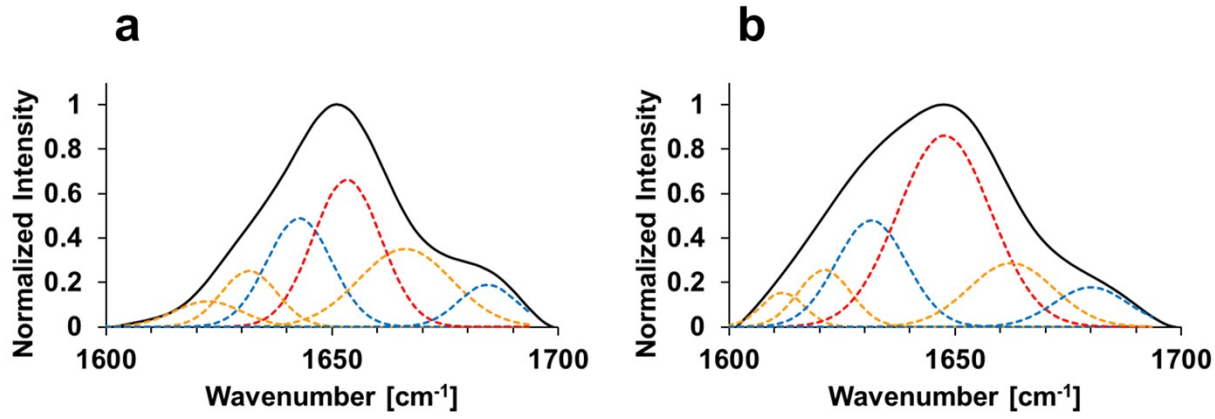

Figure S9 Representative ATR-FTIR spectral analysis of Q secondary structure in **a)** solution state and **b)** as a hydrogel. Overall spectra by deconvolution in black and individual peak deconvolutions in dotted red lines (α-helix), blue lines (β-sheet), and orange lines (random coil/turns).

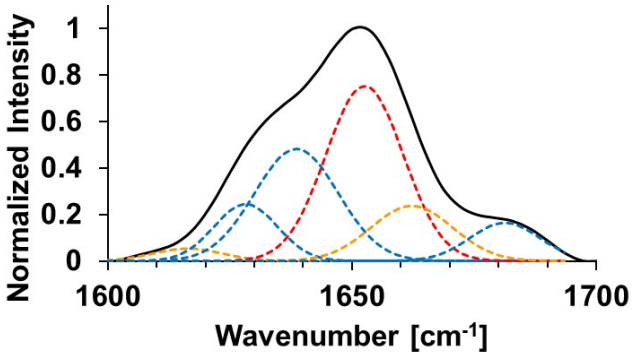

Figure S10 Representative ATR-FTIR spectral analysis of CCM-bound Q2 secondary structure. Overall spectra by deconvolution in black and individual peak deconvolutions in dotted red lines (α-helix), blue lines (β-sheet), and orange lines (random coil/turns).

Table S1. Logarithmic slopes of the mean squared displacement (MSD) of particles in the Q2 protein. Values are represented as the average and standard deviation of the passive microrheology-derived logarithmic slopes of the MSD for beads incubated with Q2 at 4 °C and measured in 12 h time intervals.

Incubation Time (h)	Logarithmic Slope of MSD ($\mu m^2 s^{-1}$)
0	1.00 ± 0.03
12	0.92 ± 0.04
24	0.57 ± 0.09
36	0.34 ± 0.08
48	0.25 ± 0.02
60	0.18 ± 0.06

Table S2. Q2 storage (G') and loss (G'') moduli from rheology under 5% oscillatory strain at 4 °C. Data is represented as the average of three independent trials.

Frequency (Hz)	G' (Pa)	G'' (Pa)

0.10	20.6	7.7
0.11	21.9	5.9
0.13	22.4	5.5
0.14	22.4	5.0
0.16	22.6	5.2
0.18	23.2	5.0
0.20	23.6	4.8
0.22	23.9	4.8
0.25	24.1	4.8
0.28	24.7	4.6
0.32	25.1	5.1
0.35	25.5	4.6
0.40	25.9	4.9
0.45	26.7	5.1
0.50	27.7	5.1
0.56	28.2	5.3
0.63	28.9	4.9
0.71	30.1	5.3
0.79	31.6	5.6
0.89	33.0	.7
1.00	35.4	5.7
1.12	37.3	5.7

1.26	39.8	6.1
1.41	42.9	6.0
1.58	45.9	6.4
1.78	49.7	6.2
2.00	54.1	6.7
2.24	58.6	6.9
2.51	64.0	7.0
2.82	69.2	7.4
3.16	75.2	7.6
3.55	81.9	8.1
3.98	89.2	9.2
4.47	99.5	9.3
5.01	110.9	10.2
5.62	125.7	10.7
6.31	144.5	12.4
7.08	168.8	13.6
7.94	200.0	15.4
8.91	239.9	17.2
10.00	289.6	20.3

Table S3. CCM-bound Q2 storage (G') and loss (G'') moduli from rheology under 5% oscillatory strain at 4 °C. Data is represented as the average of three independent trials.

Frequency (Hz)	G' (Pa)	G'' (Pa)
0.10	34.5	10.0
0.11	33.9	7.7
0.13	34.1	6.8
0.14	33.2	6.5
0.16	32.9	6.6
0.18	33.8	5.9
0.20	33.7	6.1
0.22	34.5	6.2
0.25	34.9	5.7
0.28	35.1	6.4
0.32	35.7	6.1
0.35	36.5	6.6
0.40	36.9	5.3
0.45	37.5	6.2
0.50	38.3	6.2
0.56	39.0	6.1
0.63	40.6	6.4
0.71	41.5	6.6
0.79	43.4	6.5

0.89	45.5	6.9
1.00	47.9	6.5
1.12	50.8	7.2
1.26	54.9	7.2
1.41	58.4	7.5
1.58	63.7	7.5
1.78	69.7	8.5
2.00	76.7	8.9
2.24	85.1	9.5
2.51	93.9	9.6
2.82	104.4	10.5
3.16	118.8	10.1
3.55	133.1	10.6
3.98	152.6	10.1
4.47	176.5	11.8
5.01	203.7	11.5
5.62	241.9	13.6
6.31	285.6	13.5
7.08	338.4	15.3
7.94	409.6	17.1
8.91	498.7	18.0
10.00	610.6	20.7

Table S4 ATR-FTIR compositional analysis from Q2 protein in solution and gel states. Summary of secondary structure content uses the average and standard deviation of the integrated area of deconvoluted peaks of three independent trials.

	% composition					
	α-helix	β-sheet	Antiparallel β-sheet	3-10 helix	Unordered	Aggregated Strands
Q2 Solution	28.1 ± 6.0	45.0 ± 5.6	7.1 ± 2.7	13.9 ± 1.9	0.0 ± 0.0	5.8 ± 2.3
Q2 Gel	35.8 ± 5.6	39.3 ± 2.8	8.3 ± 4.5	12.7 ± 5.8	0.0 ± 0.0	3.8 ± 3.4
Q2-CCM Gel	40.4 ± 1.0	38.3 ± 4.5	6.6 ± 1.3	13.8 ± 5.0	0.0 ± 0.0	3.5 ± 4.1
Q Solution	32.9 ± 2.4	30.6 ± 6.9	7.1 ± 0.5	24.3 ± 4.5	0.0 ± 0.0	5.2 ± 0.5
Q gel	42.8 ± 3.4	25.3 ± 5.1	6.1 ± 1.4	19.6 ± 4.8	0.0 ± 0.0	6.2 ± 4.7

References

1. L. K. Hill, M. Meleties, P. Katyal, X. Xie, E. Delgado-Fukushima, T. Jihad, C.-F. Liu, S. O'Neill, R. S. Tu, P. D. Renfrew, R. Bonneau, Y. Z. Wadghiri and J. K. Montclare, *Biomacromolecules*, 2019, **20**, 3340-3351.